Complex Systems **1** (1987) 545–558

On Lagrangian Aspects of Flow Simulation

Hassan Aref
Scott W. Jones
Department of Applied Mechanics and Engineering Science
University of California–San Diego, LaJolla, CA 92093, USA

Grétar Tryggvason
Department of Mechanical Engineering and Applied Mechanics
University of Michigan, Ann Arbor, MI 48109, USA

Abstract. Many numerical methods for fluid flow simulation use representations of the flow in terms of Lagrangian elements as opposed to Eulerian fields. Such methods have considerable advantages when they can be adapted to the physical situation in question. We show examples of this for the case of *generalized vortex* methods applied to stratified flows with sharp interfaces. We also discuss the notion of *chaotic advection*, i.e., the feature that Lagrangian elements can have chaotic motion even in Eulerian flow fields that are entirely regular. We discuss the relation of "lattice gas" methods to these issues.

1. Introduction

The abstraction of a continuous flow field of a gas or liquid from the elemental collisions of particles obeying deterministic laws of motion is a major achievement of kinetic theory and continuum mechanics. The resulting Eulerian field variables are used in most theoretical discussions of fluid mechanical phenomena. When using them, one relinquishes following individual elements of the fluid. Much as the fields of electromagnetic theory exist without a charge or current to sample them, so does the Eulerian velocity field of a fluid exist without associating specific velocities to labeled particles.

The Eulerian representation has many advantages including, in general, greater analytical tractability of the mathematical problems of fluid flow. However, once a computer is going to be doing most of the mathematical work, this consideration can become of lesser importance. Furthermore, there are in many applications Lagrangian quantities that must be monitored or calculated, and there are frequently difficulties in deriving such data reliably from purely Eulerian specifications.

The physical issues have counterparts in numerical methods seeking to exploit a Lagrangian representation of fluid flow. Sometimes a Lagrangian method is ideally suited for a particular flow situation, because the essence of the problem is the precise advection of some evolving flow feature. Examples include the recent, very successful implementations of *generalized vortex methods* to sharply stratified flows [1,2]. We pursue this aspect and show some state-of-the-art sample computations in section 3.

Lagrangian methods can appear a lot "noisier" than their Eulerian counterparts. Amsden and Harlow while pursuing a hybrid Eulerian-Lagrangian scheme, the "marker-and-cell method", remarked on "the relative orderliness of Eulerian representation over Lagrangian" [3]. This feature finds further elucidation in the topic of *chaotic advection* [4]. The trajectories of Lagrangian particles can be chaotic (in the technical sense of dynamical systems theory) even though the underlying Eulerian flow is smooth and regular. We pursue this in section 2.

This paper was prepared in connection with an interdisciplinary conference on simulation strategies for large nonlinear systems, particularly fluid flow. One of the main items discussed at this conference was the idea of "lattice gas" or "cellular automaton" models [5]. (In the context of fluid flow simulations, the former label conveys more information than the latter, and from the point of view of semantics seems preferable.) The lattice gas is a hybrid of the Eulerian and the Lagrangian representations. The "gas" aspect implies a focus on discrete particles, i.e., the conventional point of view in particle mechanics from which the Lagrangian representation is derived. The "lattice" aspect, on the other hand, immediately implies associations with the Eulerian point of view. Exactly as kinetic theory and continuum mechanics before them, current implementations of lattice gas methods lead to a Eulerian representation at the "macro-level" defining the continuum. In section 4, we comment on the relation of lattice gas models to more conventional models in use for flow simulation, with particular reference to the topics discussed in sections 2 and 3.

2. Chaotic advection

Although the field equation describing the advection and diffusion of a passive scalar field $\theta = \theta(\mathbf{x}, t)$ by a velocity field $\mathbf{V} = \mathbf{V}(\mathbf{x}, t)$, viz.

$$\frac{\partial \theta}{\partial t} + \mathbf{V} \cdot \nabla \theta = \kappa \nabla^2 \theta \tag{2.1}$$

is linear in θ, the relationship between θ and $\mathbf{V}$ is far from simple. Consider the simplest case of no diffusion, $\kappa = 0$. If we take $\theta(\mathbf{x}, t)$ to be

$$\theta(\mathbf{x}, t) = \theta_o \delta[\mathbf{x} - \mathbf{x}_o(t)], \tag{2.2}$$

we get from (2.1) that

$$\frac{d\mathbf{x}_o}{dt} = \mathbf{V}(\mathbf{x}_o t). \tag{2.3}$$

This is a system of ordinary differential equations. In three dimensions, we have

$$\dot{x}_o = u(x_o, y_o, z_o, t), \tag{2.4}$$

$$\dot{y}_o = v(x_o, y_o, z_o, t), \tag{2.5}$$

$$\dot{z}_o = w(x_o, y_o, z_o, t), \tag{2.6}$$

where (u, v, w) are the components of $\mathbf{V}$. Clearly, equations (2.3) or (2.4–6) are rich enough to admit chaotic solutions. In three dimensions, the Eulerian flow may even be steady, and chaotic particle motion can still occur [6]. In two dimensions, time dependence is necessary for chaos. A particularly simple case is two-dimensional incompressible flow. Then, we have a streamfunction $\psi(x, y, t)$ and equations (2.4), (2.5) become Hamilton's canonical equations

$$\dot{x} = \frac{\partial \psi}{\partial y}, \qquad \dot{y} = -\frac{\partial \psi}{\partial x}. \tag{2.7}$$

Configuration space for an advected particle (x, y) and the phase space of this Hamiltonian system coincide [4].

Several examples have now been studied numerically and analytically in which chaotic particle orbits ensue in flows that are regular from the Eulerian point of view [4,6,7-11]. In figure 1, we show stroboscopic Poincaré sections for a simple model flow studied recently [11]. The flow is two-dimensional and consists of alternately switching on and off a fixed point source and sink of opposite strengths. Furthermore, the fluid taken up at the sink in a given stroke is reinjected at the source during its following stroke. This simple pulsed flow results in a mapping of the plane onto itself. If we think of the plane as a complex $\mathbf{z}$ plane, and if we choose the distance between source and sink, a, as our unit length, this mapping, $\mathcal{M} : z \to z'$, is given by the equations

$$z' = \quad 1 - i\phi(-z; i\Lambda), \qquad \text{if } |z-1| < \Lambda, \tag{2.8}$$

$$z' = -1 + \phi(1 - \phi(-z; i\Lambda); \Lambda), \quad \text{if } |z-1| \geq \Lambda, \tag{2.9}$$

and

$$\phi(z; \Lambda) = (z+1)\left(1 + \frac{\Lambda^2}{|z+1|^2}\right)^{1/2}. \tag{2.10}$$

The single parameter Λ that appears in these expressions is the nondimensional ratio $Q\tau/\pi a^2$, where Q is the source strength and τ the duration of a stroke of either source or sink. Varying Λ varies the extent of the configuration space susceptible to chaos (see figure 1, panels (a), (c), and (d)).

The distributions of iterates in the various panels of figure 1 contain all the usual features of chaos in a Hamiltonian system. We note in particular

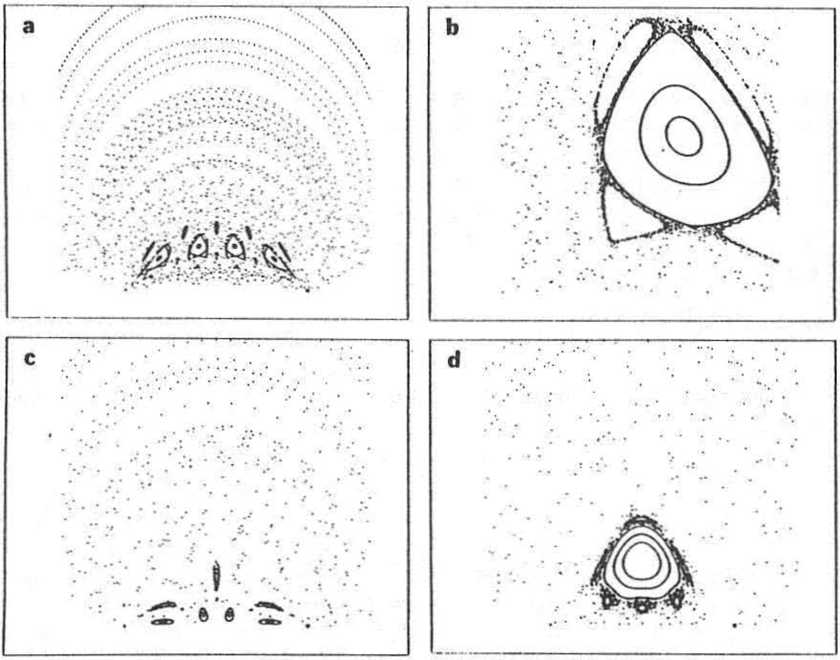

Figure 1: Stroboscopic Poincaré sections for the pulsed source-sink system studied in [11]. Panels (a), (c), and (d) are to the same scale, panel (b) is a magnification of one of the "islands" in (a) (the second from the right of the four island chain). Parameter Λ^2 is (a), (b) 0.5; (c) 1.5; (d) 3.0.

the "island chains", which in this context are accessible to direct physical observation (using a dye for example [13]). Figure 1b shows a magnification of one of the islands seen in figure 1a (the second from the left). Repeated magnifications of this type show additional structure on ever finer scales. In the absence of diffusion, this hierarchy of structure extends to arbitrarily small scales. Hence, just by *flow kinematics* a passively advected scalar can probe length scales that are orders of magnitude smaller than those over which the flow field itself varies. This aspect of advection is clearly captured by a numerical method which tracks individual particles effectively, but may be grossly miscalculated by methodologies that do not retain such Lagrangian information.

Let us turn next to another feature of the flow structure seen in figure 1. It makes a profound difference whether a blob of scalar is captured by an island or is in the "chaotic sea". We have referred to this property of chaotic advection as "sensitive dependence on initial conditions in the large" [11]. This is illustrated in figure 2, where we show two circular blobs of equal size, one started within an island of the period-4 chain seen in figure 1a, the other just outside it. As time progresses, the confining effect of the KAM curves bounding the islands is clearly seen. One circular blob is advected from island to island within the chain. The other is distributed throughout a large portion of the flow domain. Note that not too many periods of the flow are necessary for substantial differences to be visible. This type of effect must be expected for islands of all sizes in the hierarchy seen in the Poincaré sections.

What this means in terms of an accurate computation of scalar advection is that errors in the distribution of the scalar in the far subgrid resolution range of the *flow field* can amplify to errors on the order of fully resolved scales (of the flow field) in times that are of the order of a few "large eddy turnover" times. We conclude that computing Lagrangian data accurately using anything but a Lagrangian method can lead to serious errors. Diffusion of the scalar will ameliorate this situation, but has little to offer if the objective is to track discrete particles.

3. Sharply stratified flows

Another topic where the Lagrangian flow representation has been useful is in the numerical simulation of certain flows with abrupt changes in physical parameters such as density or viscosity [1,2]. This success derives from the kinematical fact that such discontinuities between immiscible fluids can be represented instantaneously as vortex sheets. With time, the sheet deforms due to the mutually induced velocities of its parts, and the vorticity evolves according to the relevant circulation theorem.

Two cases in particular have received attention from this point of view: stratified Hele-Shaw flow [2,14] and the finite amplitude Rayleigh-Taylor instability [1,15]. In both cases, the basic Lagrangian entities can be taken to be vortex elements along the interfaces. These elements carry an attribute

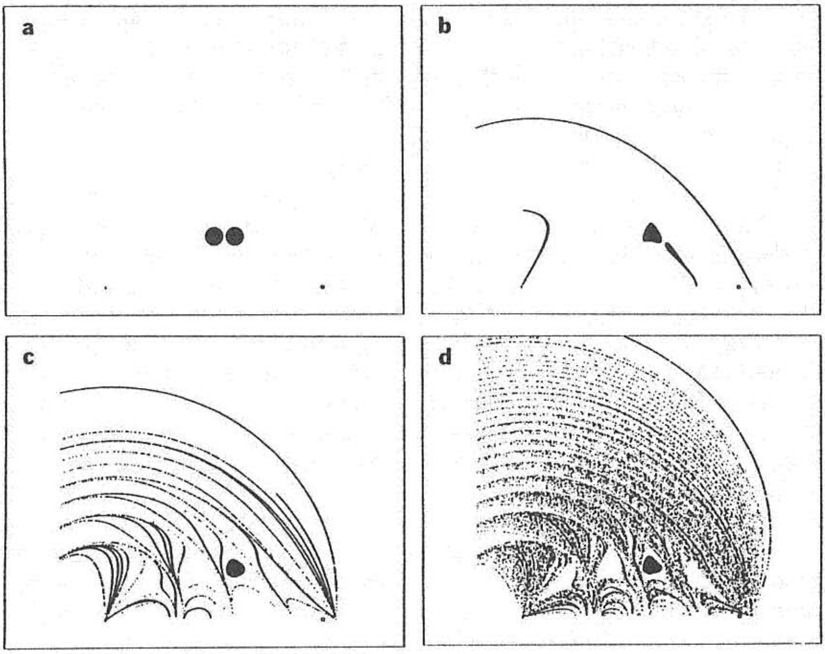

Figure 2: Sensitive dependence on initial conditions in the large for the pulsed source-sink system of figure 1 (a), (b). Two finite circular regions are initialized close to one another. Three snapshots at later times are shown. The particles in one disk remain together; those in the other disperse. The origin of this difference in behavior is seen by comparing panel (d) to figure 1(a). One disk was wholly within a KAM island, the other entirely outside it.

known as the circulation Γ.

In two dimensions, the situation is again particularly simple. An interface is then just a curve, and the incremental circulation, $\delta\Gamma$, carried by an infinitesimal element of such a curve of length δs can be written

$$\delta\Gamma = \gamma\delta s, \tag{3.1}$$

where $\gamma = \gamma(s,t)$ is called the vortex sheet strength and is the basic new quantity that enters the theory. The vortex sheet strength gives the vorticity in the flow $\omega = [0, 0, \varsigma(\mathbf{x}, t)]$ via the formula

$$\varsigma(\mathbf{x}, t) = \int \gamma(s,t)\delta[\mathbf{x} - \mathbf{x}(s,t)]d\mathbf{x}, \tag{3.2}$$

where $\mathbf{x}(s,t) = [x(s,t), y(s,t)]$ is the parametric representation in terms of arclength s of the interfacial curve at time t. Relative to the model of passive advection studied in section 2, two new features arise.

The first is that the velocity $\mathbf{V}$ now has a functional dependence on the vortex sheet strength γ. This part of the problem is kinematical, i.e., the dependence of $\mathbf{V}$ on γ is (except for the boundary conditions) independent of the physical situation. It can be expressed as an integral equation, usually associated with the name of Birkhoff, which simply inverts the relation

$$\omega = \nabla \times \mathbf{V}. \tag{3.3}$$

The second new feature is that γ itself obeys some equation of evolution. This equation comes from the momentum equation for the fluid, and thus is problem dependent.

The two particularly simple cases of *weak stratification* are worth highlighting. The first is stratified Hele-Shaw flow in the case where the fluids have different densities but negligibly different viscosities. In terms of nondimensional variables, explained in more detail elsewhere [2], the equation for γ (in the absence of interfacial surface tension; see below) is

$$\gamma = \frac{\partial y}{\partial s}, \tag{3.4}$$

where y is the vertical coordinate of the interface (gravity is directed in the negative y-direction). In terms of the incremental circulation $\delta\Gamma$, equation (3.1), the formula is

$$\delta\Gamma = \delta y. \tag{3.5}$$

The second case is weakly stratified Rayleigh-Taylor flow, where the density difference between the two layers of superimposed fluid is slight. Scaling and nondimensionalization in the so-called *Boussinesq limit* gives the equation

$$\frac{d(\delta\Gamma)}{dt} = \delta y. \tag{3.6}$$

(The nondimensionalization is different in (3.5) and (3.6)).

For both problems (3.5) and (3.6), it is in general necessary to provide a stabilizing mechanism for the smallest scales. In the absence of such "regularization", both models have instabilities for a flat, horizontal interface with growth rates which increase with decreasing wavelength. The nonlinear extension of this feature can lead to a singularity forming in a finite time even when the flow starts from a smooth initial condition such as a sine wave [16,17].

A physically motivated regularization is to introduce interfacial surface tension. This adds a term of the form $B\delta\kappa$ to the right-hand side of equations (3.5) and (3.6), where B is a nondimensional version of the surface tension, and κ is the local interfacial curvature. For Hele-Shaw flow, it appears that addition of surface tension is indeed sufficient to regularize the evolution. For Rayleigh-Taylor flow, computational experience suggests that this is not the case. This can be rationalized since surface tension is a dissipative mechanism with the dynamics (3.5) but a dispersive mechanism for equation (3.6). Hence, perturbations will be damped out by adding surface tension to equation (3.5) but will lead to capillary waves when added to equation (3.6). For a weakly stratified Rayleigh-Taylor interface, reliable simulations can be produced by introducing various numerical regularization procedures in much the same way as can be done for the Kelvin-Helmholtz roll-up of a vortex sheet [18,19].

We stress that equations (3.5) and (3.6) are simplified limiting forms. For the general case of stratified Hele-Shaw flow, i.e., for fluids of different viscosities as well as densities, the equation for γ is a Fredholm integral equation of the second kind [2]. For the general case of the inviscid Rayleigh-Taylor problem, i.e., for fluids of different densities, the equation for γ is an integro-differential equation [1]. Numerical implementations of the simple models (3.5) and (3.6) are not much more difficult than implementations of standard vortex methods for inviscid flow (where the equation for $\delta\Gamma$, by Kelvin's circulation theorem, is that $d(\delta\Gamma)/dt = 0$). Computational experience shows that the Hele-Shaw problem can be calculated convincingly for arbitrary viscosity stratification [2], whereas the Rayleigh-Taylor problem is well under control only in the Boussinesq limit and in the limit where one fluid is replaced by a vacuum [1,15].

In figure 3, we show representative calculations of a subharmonic instability of an interface in stratified Hele-Shaw flow (in both cases using dynamics more complicated than the weakly stratified limit (3.5)). Two cases are shown. In both cases, the bottom fluid is lighter and less viscous than the top fluid. In the upper sequence, the bottom fluid is assumed to have negligible viscosity compared to the top fluid. In the lower three-panel sequence, the ratio of viscosities is 1:3. The interface initially was perturbed by two waves, one at the most amplified wavelength (according to linear stability theory for a flat interface), the other at three times that wavelength. Although the shorter wave has a larger growth rate according to linear theory, and alone would lead to three identical bubbles or "fingers" at long times, there is a nonlinear selection mechanism that comes about from the interactions of the developing fingers. In the large amplitude limit, the long wave modulation wins and only one bubble ensues. Thus, in figure 3, we see two effects. One is the sensitive dependence on initial conditions for given flow parameters seen if either sequence in figure 3 is compared to the three-finger evolution that would have taken place if the longer wave were not present in the initial state. The other is the dependence for a fixed initial state on global flow parameters, here the viscosity ratio. This is seen by simply comparing the two sequences in figure 3 panel by panel.

In figure 4, we show stages in the evolution of a multi-wavelength initial perturbation to a Rayleigh-Taylor unstable interface in the Boussinesq limit. The characteristic vortex pair "mushrooms" are clearly visible. At large amplitudes, very complicated interactions take place among these structures. At lower numerical resolution, the large scales of the flow structures are retained, but the intricate spirals in the roll-up are obliterated. For some processes, such as mixing and chemical reactions, it is important to have accurate information on these finer scale features.

Two points emerge from these examples that are in some ways quite similar to those made in section 2. First, we have seen in figure 3 the sensitivity at long times to modes present in the initial state even with very small amplitudes. The longer wavelength perturbation to the flat interface has an almost indiscernible amplitude relative to the shorter wavelength, yet it dominates at late times. The qualitative physics of this is readily understandable using standard ideas of mode competition and growth. A numerical method that attempts to simulate this flow situation must resolve such competition effects. For example, a method that introduces spurious long-wave behavior would fail. In the second example, figure 4, we again see the evolution of structure on much smaller scales than one might have guessed from the initial state. The main issue here is the reliable prediction of such structure for a given expenditure of computational resources.

4. Conclusions

We have given several examples where the flow physics suggests that a Lagrangian representation is advantageous both theoretically and computationally. We have shown in these examples the delicate and sensitive nature of the dependence of flow quantities at long times on small changes in initial conditions. We have seen also examples of the more familiar sensitivity to the values of global flow parameters, such as Λ in the pulsed source-sink system or the viscosity ratio across the interface in stratified Hele-Shaw flow.

The examples discussed in sections 2 and 3 were chosen in part because they highlight areas where general-purpose numerical methods are likely to have difficulties. Tracking such features as arbitrarily fine-grained, ramified spatial structure or the competition between small differences in initial amplitude of different wave modes required methods which do not introduce

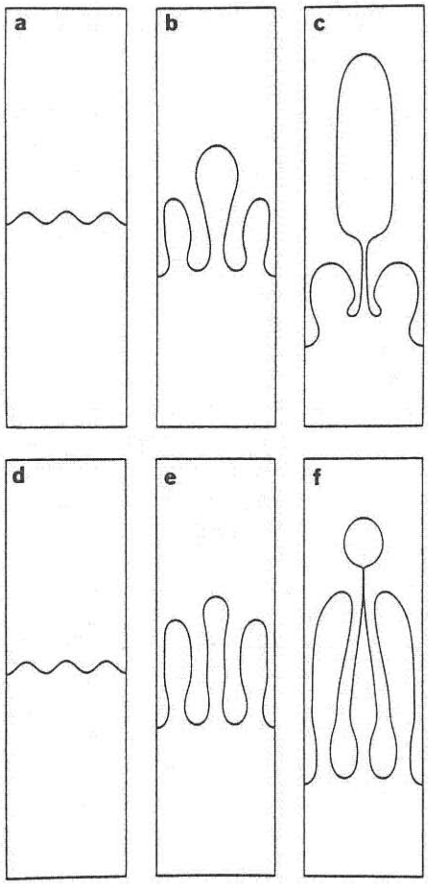

Figure 3: Growth of small amplitude subharmonic on a sharp interface in stratified Hele-Shaw flow. The clearly visible wave is at the most amplified wavelength according to linear stability theory. The low amplitude wave has a much smaller amplitude. As the flow evolves, the longer wave dominates and one finger emerges ahead of the other two. In the upper sequence (a–c), the bottom fluid has negligible viscosity. In the lower sequence, the viscosity ratio between bottom and top fluids is 1:3.

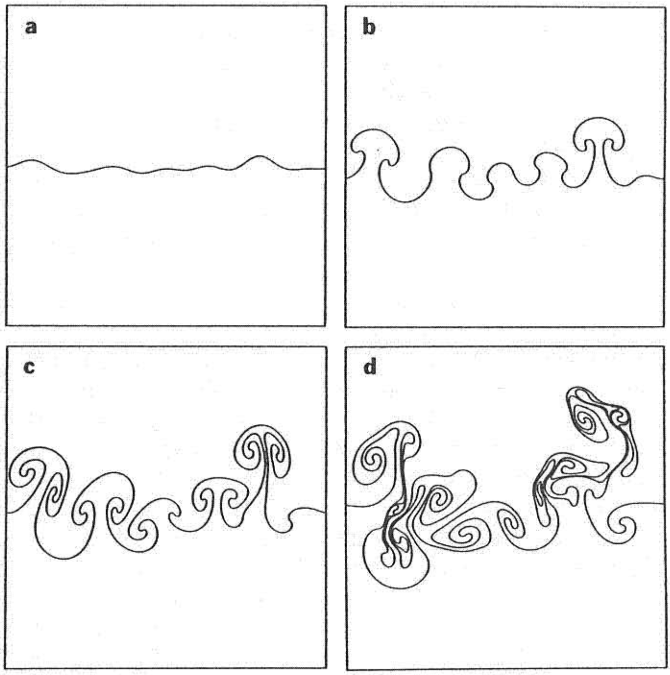

Figure 4: A sequence of configurations of a weakly stratified, Rayleigh-Taylor unstable interface computed by a generalized vortex method. The initial perturbation was an arbitrarily chosen superposition of waves. Highly convoluted, fine-scale structure emerges as the interface evolves.

numerical diffusion and for which fluctuations are extremely well controlled. We are particularly concerned here about the potential of lattice gas models of fluid flow in these respects.

Of the examples that we have discussed, the only one that has been attempted by lattice gas methods (as far as we are aware) is the Rayleigh-Taylor instability in the Boussinesq limit [20]. The results presented in the last two panels of figure 4 appear to be well beyond the reach of lattice gas methods and are, indeed, beyond what most general-purpose and many special-purpose methods can achieve at the present time.

The chaotic advection examples are in principle so simple ("just kinematics") that standard computational methods for fluid flows would consider them an insult. However, they raise some very fundamental issues, since they require explicitly the numerical simulation of chaotic orbits of a simple dynamical system here given by the stroboscopic mapping. When scrutinized at a fundamental level, this is a highly nontrivial task [21].

From an operational standpoint, the main problem facing lattice gas methods seems to be the enhanced level of fluctuations from an artificially amplified "microworld". Would a lattice gas model of stratified Hele-Shaw flow, for example, be able to reproduce the amplitude dependence demonstrated in figure 3? Would it even retain the left-right symmetry? The models of this general type that have been advanced so far, such as percolation models or "diffusion limited aggregation" [22], certainly do not appear to have such sensitivity.

From a more general point of view, it seems to us that most special-purpose algorithms for flow simulation attempt to incorporate a substantial amount of flow physics. The generalized vortex methods provide an example of this trend, but we might mention also other front-tracking methods where the solution of a Riemann problem for each of a range of different situations is included in a fairly general code framework [23]. Given a required level of detail and a general-purpose algorithm for fluid flow, it is probably possible to find a situation where any reasonable implementation of that algorithm will fail to produce reliable answers. This provides the impetus for seeking out special-purpose algorithms and methods. Conversely, new methodologies touted as "general" invariably define some range of problems where they outperform competing methods. They survive by exploiting and expanding that initial range of success. Lattice gas methods must still establish such a niche for themselves.

Acknowledgments

We are indebted to A. Pumir, R. Teigland, and O. M. Thomas for discussion. This work is supported in part by the DoE, Office of Basic Energy Sciences; DARPA, Applied and Computational Mathematics Program; and an NSF/PYI award. Matching funds for the latter have been provided by General Electric Co., CRAY Research, Ametek Computer Research Division, and the Petroleum Research Fund of the American Chemical Society.

Computing resources at the San Diego Supercomputer Center have been invaluable.

References

[1] G. R. Baker, D. I. Meiron, and S. A. Orszag, *Physics of Fluids*, **23** (1980) 1485; *Journal of Fluid Mechanics*, **123** (1982) 477.

[2] G. Tryggvason and H. Aref, *Journal of Fluid Mechanics*, **136** (1983) 1; **154** (1985) 287.

[3] A. A. Amsden and F. H. Harlow, *Physics of Fluids*, **7** (1964) 327.

[4] H. Aref, *Journal of Fluid Mechanics*, **143** (1984) 1.

[5] U. Frisch, B. Hasslacher, and Y. Pomeau, *Physical Review Letters*, **56** (1986) 1505.

[6] T. Dombre, U. Frisch, J. M. Greene, M. Hénon, A. Mehr, and A. M. Soward, *Journal of Fluid Mechanics*, **167** (1986) 353.

[7] H. Aref and S. Balachandar, *Physics of Fluids*, **29** (1986) 3515.

[8] J. Chaiken, C. K. Chu, M. Tabor, and Q. M. Tan, *Physics of Fluids*, **30** (1987) 687.

[9] L. A. Smith and E. A. Spiegel, *Lecture Notes in Physics*, **230** (1986) 306.

[10] D. V. Khakhar, H. Rising, and J. M. Ottino, *Journal of Fluid Mechanics*, **172** (1986) 419.

[11] S. W. Jones and H. Aref, submitted to *Physics of Fluids*.

[12] W. L. Chien, H. Rising, and J. M. Ottino, *Journal of Fluid Mechanics*, **170** (1986) 355.

[13] J. Chaiken, R. Chevray, M. Tabor, and Q. M. Tan, *Proceedings of the Royal Society London, Ser. A*, **408** (1986) 165.

[14] A. J. DeGregoria and L. W. Schwartz, *Journal of Fluid Mechanics*, **164** (1986) 383.

[15] G. Tryggvason, Proc. UC Davis INLS Workshop on CFD (July 1986), *Journal of Computational Physics*, in press.

[16] D. W. Moore, *Proceedings of the Royal Society London, Ser. A*, **365** (1979) 105.

[17] D. I. Meiron, G. R. Baker, and S. A. Orszag, *Journal of Fluid Mechanics*, **114** (1982) 283.

[18] R. Krasny, *Journal of Computational Physics*, **65** (1986) 292.

[19] G. Tryggvason, Proc. SIAM Workshop on Multiphase Flow, Lessburg, VA (June 1986), *Journal of Computational Physics*, in press.

[20] D. d'Humières and P. Lallemand, "Numerical Simulations of Hydrodynamics with Lattice Gas Automata in Two Dimensions", *Complex Systems*, **1** (1987) 598.

[21] J. L. McCauley, Jr., and J. I. Palmore, *Physics Letters A*, **115** (1986) 433.

[22] T. A. Witten and L. M. Sander, *Physical Review Letters*, **47** (1981) 1400; *Physical Review B*, **27** (1983) 5686.

[23] J. Glimm, E. Isaacson, D. Marchesin, and D. McBryan, *Advances in Applied Math*, **2** (1981) 91.